RSC Advances

ROYAL SOCIETY OF CHEMISTRY

www.rsc.org/advances

Journal Name

ARTICLE

A fluorescent chemsensor based on imidazo[1,2-a]quinoline for Al^{3+} and Zn^{2+} in respective solutions

Received 00th January 20xx,
Accepted 00th January 20xx

DOI: 10.1039/x0xx00000x

www.rsc.org/

Junhua Sun, Zheng Liu, Ying Wang, Shihua Xiao, Meishan Pei, Xiuxian Zhao, and Guangyou Zhang*

A new chemsensor N'-[(2-hydroxyphenyl)methylidene]imidazo[1,2-a]quinoline-2-carbohydrazide (**L2**) was developed which could detect Al^{3+} in DMSO/H_2O HEPES buffer and detect Zn^{2+} in EtOH/H_2O HEPES buffer. The chemsensor exhibits high selectivity and sensitivity for sensing Al^{3+} and Zn^{2+} with a fluorescense "turn-on" mode.

Introduction

Serving as the most abundant metal on earth and the second most abundant transition metal in human body, aluminium and zinc carry irreplaceable weight in livings. As a potential toxic ion, aluminium is a non-essential element for biological processes that has been implicated in various neurodegenerative and neurological disorders, such as Alzheimer's disease, dialysis encephalopathy, and problems in bone, muscles, etc[1-3]. According to WHO (World Health Organization) report, the average daily intake of aluminium is approximately 3-10 mg per day for human beings, which has been widely used in food additive, aluminium-based pharmaceuticals, and aluminium containers and cooking utensils[4]. Zinc is an essential element for life and plays critical roles in many biochemical processes, such as gene expression, apoptosis, immune system response and neurotransmission[5-8]. However, the disordered cellular zinc level can induce various diseases, for instance, Alzheimer's disease, epilepsy and infantile diarrhea[9-10]. Consequently, the recognition and quantification of aluminium and zinc ions are significant goals in both biological and environmental research fields.

With regard to the detection of environmentally and biologically relevant ions, fluorescence measurement is considered to be a versatile technique with high sensitivity, rapid response, and easy performance [11-12]. In particular, molecular chemosensors that show fluorescence responses upon selective binding with metal ions have received great interest since it is cost-effective, rapid, real time-monitoring and facile[13]. In recent years, the fluorescent chemsensors for the detection of zinc[14-20] or aluminium ions[21-24] are emerging continually. But most of fluorescence chemosensors are studies in single organic solvents, such as THF, DMSO and EtOH, etc. So far, the effect of different solvents on chemosensors for the selective and sensitive metal-ion detection has been rarely reported[25]. Therefore, there is still a urgent need to develop new sensors that render to recognize different metal ions selectively in dependent solvent. Based on the above needs and the studies about quinoline-based ligands[26-33], a new and simple sensor (**L2**) for Al^{3+} and Zn^{2+} was designed and synthesized (Scheme 1), which show distinctly different optical properties in different solvent systems. Sensor **L2** exhibits enhanced fluorescence with high selectivity upon binding to Al^{3+} in DMSO/H_2O HEPES buffer, but to Zn^{2+} in EtOH/H_2O HEPES buffer.

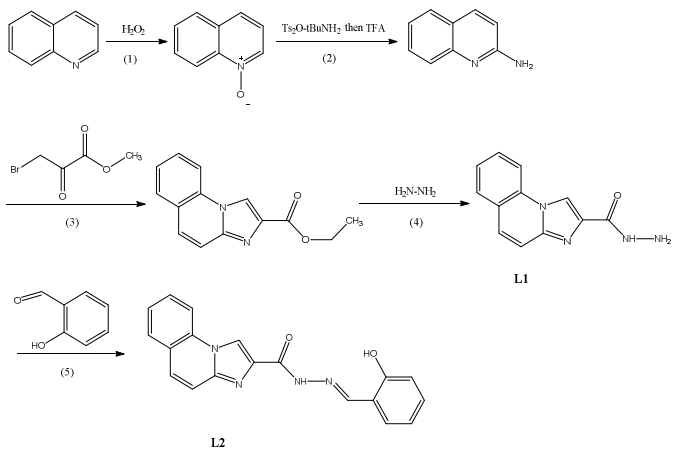

Scheme 1 Synthetic route of **L1** and **L2**. Conditions: (1) CH_3CN, catalyst MoO_3, H_3PO_4, at 50°C for 12h; (2) benzotrifluoride, at 70°C for 5h; (3) THF, reflux for 16h; (4) MeOH, at room temperature for 1h; (5) EtOH, at room temperature for 12h.

School of Chemistry and Chemical Engineering, University of Jinan, Jinan 250022, China. E-mail: chm_zhanggy@ujn.edu.cn; Tel: +86-13296449182
Electronic Supplementary Information (ESI) available. See DOI: 10.1039/x0xx00000x

Experimental section

Materials and instruments

All organic reagents were obtained from commercial suppliers and used without purification. UV-vis spectra were recorded on a Shimadzu 3100 spectrometer. Fluorescence measurements were carried out using Edinburgh Instruments Ltd-FLS920 fluorescence spectrophotometer. ^{1}H NMR spectra were recorded on Bruker AV III 400 MHz NMR spectrometer and ^{13}C NMR spectra were recorded on a Bruker AV III 100 MHz NMR spectrometer with tetramethysilane (TMS) as an internal standard. Infrared spectra were recorded using a Bruker Vertex 70 FT-IR spectrometer with KBr pellets.

Methods for the preraration of the receptor

Synthesis of compound imidazo[1,2-a]quinoline-2-carbohydrazide (L1) The compoud **L** (ethyl imidazo[1,2-a]quinoline-2-carboxylate) was synthesized following a series of previously reported methods[34-36]. Hydrazine hydrate (80%, 4 mL) was added dropwise to methanol solution (20 mL) of ethyl imidazo[1,2-a]quinoline-2-carboxylate (0.91 mmol, 0.22 g). The reaction mixture was stirred for 12 h at room temperature. Solvent was then removed under reduced pressure, and the residue was dissolved in chloroform (10 ml). The organic layer was washed with water, dried over anhydrous Na_2SO_4, filtered, and condensed. The residue was purified by silica gel chromatography with chloroform /methanol (v/v, 15:1) as developing solvent to give compound **L1** as gray solid (0.16 g, 77%). ^{1}H NMR [400 MHz, DMSO-d_6, J=Hz, δ (ppm)]: 9.58 (1 H, s), 9.16 (1 H, s), 8.50 (1 H, d, J=8.4), 8.01 (1 H, dd, J=7.9, 1.2), 7.76 (2 H, ddd, J=12.3, 9.7, 5.5), 7.61–7.51 (2 H, m), 4.56 (2 H, s).^{13}C NMR [101 MHz, DMSO, δ (ppm)]: 161.81, 142.99, 138.78, 132.86, 129.93, 129.63, 128.13, 126.03, 123.42, 117.14, 116.74, 114.76. $[M+H]^+$: 227.1.

Synthesis of compound N'-[(1E)-(2-hydroxyphenyl)methylidene] imidazo[1,2-a]quinolie-2-carbohydrazide (L2) Salicylic aldehyde (0.98 mmol, 0.12 g) was added to an ethanol solution (30 mL) of imidazo[1,2-a]quinoline-2-carbohydrazide (0.43 mmol, 0.10 g). Then the solution was stirred for 12 h at room temperature and white precipitate appeared. The precipitate was filtered and then washed with ethanol to isolate **L2** in pure form (0.09 g, 62%); ^{1}H NMR [400 MHz, DMSO-d_6, J=Hz, δ (ppm)]: 12.39 (1 H, s), 11.51 (1 H, s), 9.38 (1 H, s), 8.80 (1 H, s), 8.59 (1 H, d, J=8.3), 8.05 (1 H, d, J=7.9), 7.87 (1 H, d, J=9.6), 7.78 (1 H, t, J=7.8), 7.62 (2 H, dd, J=12.6, 5.9), 7.47 (1 H, d, J=8.0), 7.32 (1 H, t, J=7.8), 6.94 (2 H, t, J=7.6). ^{13}C NMR [101 MHz, DMSO, δ (ppm)]: 158.85, 158.03, 149.41, 143.17, 137.98, 132.84, 131.75, 130.37, 130.11, 129.72, 128.74, 126.36, 123.52, 119.81, 119.13, 117.02, 116.93, 116.67. ESI-MS: $[M+H]^+$: 331.1.

Preparation of test solution

Stock solutions of the probe **L2** (2.0×10^{-5} M) were prepared in two solvent systems: DMSO/H_2O HEPES buffer (10 mM, pH=7.4, 9:1, v/v) , EtOH/H_2O HEPES buffer (10 mM, pH=7.4, 9:1, v/v). Stock solutions of various ions were prepared in deionized water.

Results and discussion

The properties of L2 in DMSO/H_2O HEPES buffer

As shown in Fig. S9, the complexation time in the system of DMSO/H_2O HEPES buffer (10 mM, pH=7.4, 9:1, v/v) was investigated by monitoring the fluorescent emission intensity of **L2** (20 μ M) bonding with Al^{3+} (10 equiv.) at an excitation wavelength of 305 nm. After the addition of Al^{3+}, the fluorescent intensity of **L2** at λ=450 nm was enhanced to a relatively stable value after 6 h. Therefore, the complexation time of 6 h was used for this system.

The selectivity of **L2** for different metal ions (Cu^{2+}, Ag^{+}, Cd^{2+}, Hg^{2+}, Na^{+}, K^{+}, Co^{2+}, Pb^{2+}, Mn^{2+}, Li^{+}, Ni^{2+}, Fe^{3+}, Ca^{2+}, Cr^{3+}, Zn^{2+}, Mg^{2+}, Al^{3+}) was investigated by fluorescence emission spectroscopy. **L2** (20 μ M) exhibited a weak fluorescence intensity at 375 nm when it was excited at 305 nm in DMSO/H_2O HEPES buffer (10 mM, pH=7.4, 9:1, v/v). The addition of Al^{3+} to the solution induced a remarkable increase in the fluorescence intensity along with a significant red shift of 75 nm (Fig. 1A). Meanwhile, there was a sharp change from colorless to blue in the presence of Al^{3+} ions (Fig. 1A inset). In contrast, addition of other metal ions caused almost negligible fluorescence increase. To further understand the properties of **L2** as a receptor for Al^{3+}, a titration experiment was performed with increasing concentration of Al^{3+} (Fig. 1B). Upon incremental addition of Al^{3+}, the fluorescence emission maximum at 450 nm gradually increased and reached a plateau when the concentration of Al^{3+} was 25 equiv.. The fluorescence intensity of **L2** (20 μ M) at λ=450 nm increased linearly with the concentration of Al^{3+} from 1 up to 10 μ M. A good linear relationship was observed between the fluorescence intensity and $[Al^{3+}]$ (Fig. S10). The detection limit (3σ/slope) for Al^{3+} was calculated to be 1.73×10^{-7} M. The fluorescence quantum yield of **L2** in DMSO/H_2O HEPES buffer was 0.36 and was increased to 0.77 by Al^{3+} addition.

To further check the selectivity of receptor **L2** towards Al^{3+}, competitive experiment was carried out in DMSO/H_2O HEPES buffer (10 mM, pH=7.4, 9:1, v/v). When **L2** was treated with 1 equiv. of Al^{3+} in the presence of the same concentration of other metal ions (Fig. S12), several metal ions (Ni^{2+},Cu^{2+} and Cd^{2+}) decreased the emission intensity and some other metal ions (Pb^{2+}, Fe^{3+}, Zn^{2+} and Mg^{2+}) increased the emission intensity obviously. Even so, the result of Fig. 1A had confirmed the solely addition of other metal ions caused no significant florescence increase.Thus, **L2** can be used potentially to qualitatively detect Al^{3+} in specified condition.

The UV-vis spectrum of **L2** in DMSO/H_2O HEPES buffer (20 μ M) in the prescence of 10 equiv. of a variety of metal ions (Cu^{2+}, Ag^{+}, Cd^{2+}, Hg^{2+}, Na^{+}, K^{+}, Co^{2+}, Pb^{2+}, Mn^{2+}, Li^{+}, Ni^{2+}, Fe^{3+}, Ca^{2+}, Cr^{3+}, Zn^{2+}, Mg^{2+}, Al^{3+}) was detected as shown in Fig. S14. The result show that these metal ions (Fe^{3+}, Ni^{2+}, Cu^{2+}) could be distinguished easily over other ones using UV-vis spectroscopy. In addition, the activity of **L2** toward Al^{3+} was

examined solely with absorption spectroscopy. The sensor **L2** displayed four characteristic peaks at 291, 301, 326 and 339 nm in DMSO/H_2O HEPES buffer (10 mM, pH=7.4, 9:1, v/v).

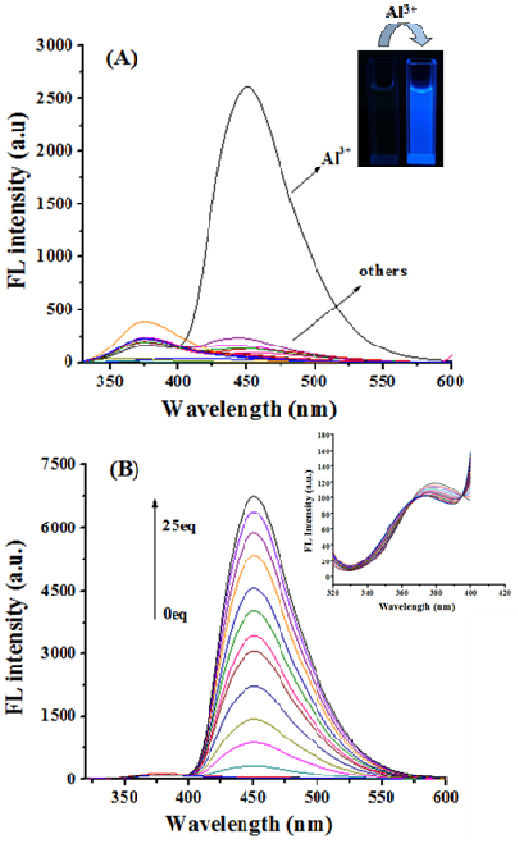

Fig. 1 (A) Fluorescence spectra of **L2** (20 μ M) upon the addition of metal salts (10equiv.) of Cu^{2+}, Ag^{+}, Cd^{2+}, Hg^{2+}, Na^{+}, K^{+}, Co^{2+}, Pb^{2+}, Mn^{2+}, Li^{+}, Ni^{2+}, Fe^{3+}, Ca^{2+}, Cr^{3+}, Zn^{2+}, Mg^{2+}, and Al^{3+} in DMSO/H_2O HEPES buffer (10 mM, pH=7.4, 9:1, v/v). λ ex=305nm.Inset: color of **L2** and **L2**+Al^{3+} system under UV lamp. (B) Fluorescence titration spectra of **L2** (20 μ M) upon an incremental addition of Al^{3+} (up to 25equiv.) in DMSO/H_2O HEPES buffer (10 mM, pH=7.4, 9:1, v/v). λ ex=305nm.

Titration experiments with incremental addition of Al^{3+} ions resulted in the decline of the four intrinsic peaks along with the emergence of two new peak at 382 nm and 407 nm. A distinct isosbestic point at 354 nm implied the complete conversion of **L2** to its Al^{3+} complex (Fig. 2). To confirm the chelation structure, DFT calculations were carried out with B3LYP/6-31G(d) basis sets using a suite of Gaussian 09 programs. Structure optimization and energy calculations provide the best binding mode between **L2** and Al^{3+} (Fig. 3). The DFT calculations also revealed that there is a reasonable decrease in the HOMO to LOMO energy gap from **L2** to its aluminium complex (Fig. 4), which is consistent with the emerging of the new red shifted absorbance peaks on the addition of Al^{3+} to **L2**.

The effect of pH was studied dependently. Over the pH range tested, **L2** has nearly no fluorescence. Sharp decline was observed at acidic (pH < 7) and basic (pH > 8) conditions in presence of Al^{3+}. At lower pH (2-7), the decline probably attribute to the protonation of the imidazole nitrogen, which interfere the coordination between metal ions and the nitrogen. At pH greater than 8, the fall of the fluorescence intensity possibly due to formation of salt.

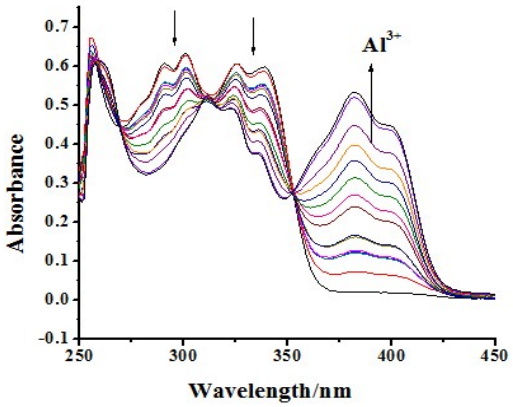

Fig. 2 Changes in absorption spectra of **L2** (20 μ M) with the incremental addition of Al^{3+} in DMSO/H_2O HEPES buffer (10 mM, pH=7.4, 9:1, v/v).

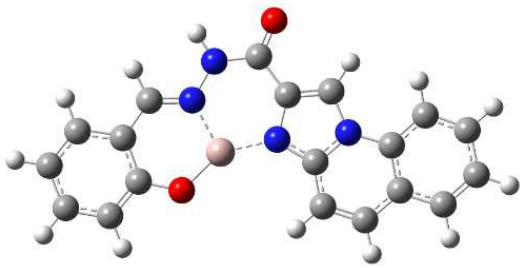

Fig. 3 Optimized structure of **L2**+Al^{3+} at B3LYP/6-31+ G(d,p)

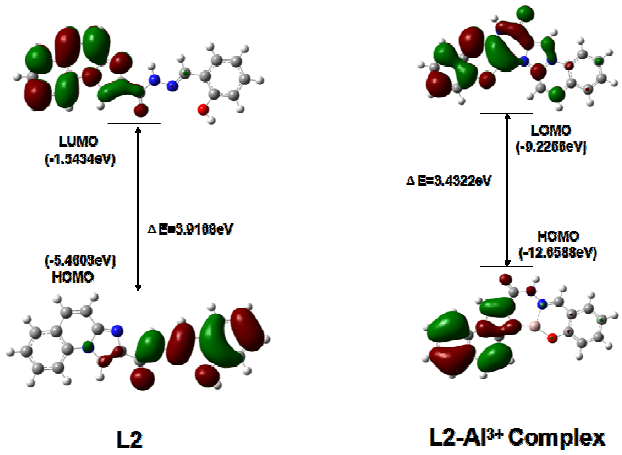

Fig. 4 Energy diagrams of HOMO and LOMO orbitals of **L2** and **L2**+Al^{3+} complex calculated at the DFT level using a B3LYP/6-31G(d) basis set within the Gaussian 09 programs.

The properties of L2 in EtOH/H_2O HEPES buffer

The complexation time in the system of EtOH/H_2O HEPES buffer was very short which can be ignored. The selectivity of **L2** for different metal ions (Cu^{2+}, Ag^{+}, Cd^{2+}, Hg^{2+}, Na^{+}, K^{+}, Co^{2+}, Pb^{2+}, Mn^{2+}, Li^{+}, Ni^{2+}, Fe^{3+}, Ca^{2+}, Cr^{3+}, Zn^{2+}, Mg^{2+}, Al^{3+}) in EtOH/H_2O HEPES buffer was detected by fluorescence spectra. As is evident from Fig. 5A, a solution of **L2** (20 μM) showed a low intensity at 345 nm when it was excited at 315 nm in EtOH/H_2O HEPES buffer (10 mM, pH=7.4, 9:1, v/v). The addition of Zn^{2+} to the solution induced a large increase in the fluorescence intensity, along with a significant red shift of 144 nm. There was also a dramatic color change from colorless to yellow green in the presence of Zn^{2+} ions (Fig. 5A inset). While other metal ions induced unconspicuous fluorescence increase. Similarly, fluorescent titration was also conducted (Fig. 5B). Upon incremental addition of Zn^{2+}, the fluorescence emission maximum at 489 nm gradually increased and reached a plateau when the concentration of Zn^{2+} was 7 equiv.The fluorescence intensity of **L2** (20 μM) at λ=489 nm increased linearly with the concentration of Zn^{2+} from 0.1 up to 1 μM. A good linear relationship was observed between the fluorescence intensity and [Zn^{2+}] (Fig. S11). The detection limit (3σ/slope) for Zn^{2+} was calculated to be 6.36×10^{-8} M. The fluorescence quantum yield of **L2** in EtOH/H_2O HEPES buffer was 0.25 and was increased to 0.41 by Zn^{2+} addition.

Competitive experiment was carried out in EtOH/H_2O HEPES buffer (10 mM, pH=7.4, 9:1, v/v). When **L2** was treated with 1 equiv. of Zn^{2+} in the presence of the same concentration of other metal ions (Fig. S13), several metal ions (Ni^{2+}, Fe^{3+} and Cu^{2+}) decreased the emission intensity and most of the metal ions (Pb^{2+}, Co^{2+}, Ag^{+}, Hg^{2+}, Al^{3+}, Cr^{3+} and Mg^{2+}) increased the emission intensity. Nonetheless, the result of Fig. 5A had confirmed the solely addition of other metal ions caused no significant florescence enhancement. Thus, **L2** can be used potentially to qualitatively detect Zn^{2+} in specified condition.

The UV-vis spectrum of **L2** (20 μM) in EtOH/H_2O HEPES buffer (10 mM, pH=7.4, 9:1, v/v) in the prescence of 7 equiv. of a variety of metal ions (Cu^{2+}, Ag^{+}, Cd^{2+}, Hg^{2+}, Na^{+}, K^{+}, Co^{2+}, Pb^{2+}, Mn^{2+}, Li^{+}, Ni^{2+}, Fe^{3+}, Ca^{2+}, Cr^{3+}, Zn^{2+}, Mg^{2+}, Al^{3+}) was detected as shown in Fig. S15. It is not easy to differentiate various metal ions using UV-vis spectroscopy. The UV-spectra properties of **L2** and **L2**+Zn^{2+} were researched in EtOH/H_2O HEPES buffer. The receptor **L2** also has four absorption peaks respectively at 290, 298, 322, and 333 nm in EtOH/H_2O HEPES buffer, which is similar with **L2** in DMSO/H_2O HEPES buffer.

Titration experiments with incremental amounts of Zn^{2+} ions resulted in the decreasing of the four intrinsic peaks along with the emergence of a new peak at 390 nm. A distinct isosbestic point at 354 nm established the transformation of a free receptor in its zinc complex (Fig. 6). The DFT calculations of **L2**+Zn^{2+} have similar results with **L2**+Al^{3+} (Fig. 7 and Fig. 8).

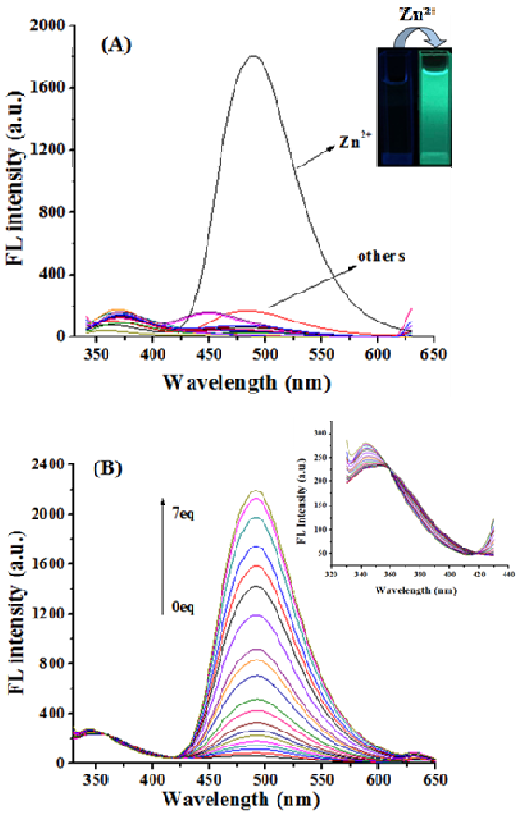

Fig. 5 (A) Fluorescence spectra of **L2** (20 μM) upon the addition of metal salts (7 equiv.) of Cu^{2+}, Ag^{+}, Cd^{2+}, Hg^{2+}, Na^{+}, K^{+}, Co^{2+}, Pb^{2+}, Mn^{2+}, Li^{+}, Ni^{2+}, Fe^{3+}, Ca^{2+}, Cr^{3+}, Zn^{2+}, Mg^{2+}, Al^{3+} in EtOH/H_2O HEPES buffer (10 mM, pH=7.4, 9:1, v/v). λ ex=315nm. Inset: color of **L2** and **L2**+Zn^{2+} system under UV lamp. (B) Fluorescence titration spectra of **L2** (20 μM) upon an incremental addition of Zn^{2+} (up to 7 equiv.) in EtOH/H_2O HEPES buffer (10 mM, pH=7.4, 9:1, v/v). λ ex=315nm.

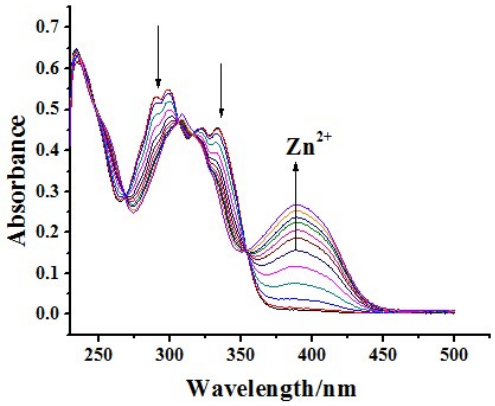

Fig. 6 Changes in absorption spectra of **L2** (20 μ M) with the incremental addition of Zn^{2+} in EtOH/H_2O HEPES buffer (10 mM, pH=7.4, 9:1, v/v).

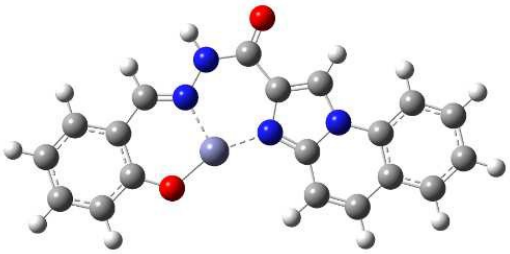

Fig. 7 Optimized structure of **L2**+Zn^{2+} at B3LYP/6-31+ G(d,p)

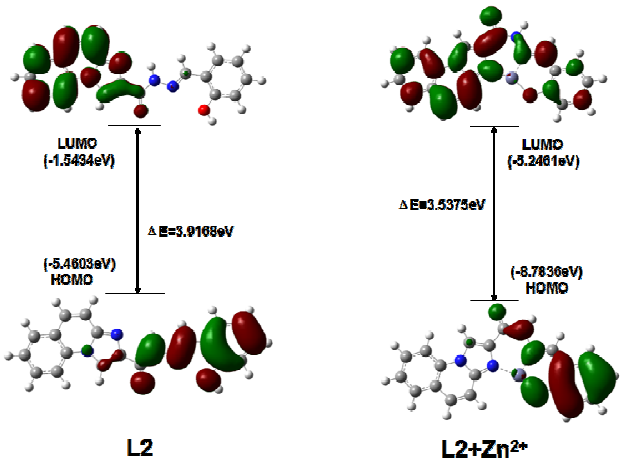

Fig. 8 Energy diagrams of HOMO and LOMO orbitals of **L2** and **L2**+Zn^{2+} complex calculated at the DFT level using a B3LYP/6-31G(d) basis set within the Gaussian 09 programs.

The fluorescence changes of **L2** (20 μ M) in the absence and presence of Zn^{2+} in different pH values were examined. The influence of pH for **L2** and **L2**+Zn^{2+} in EtOH/H_2O solution was analogous to **L2** and **L2**+Al^{3+} in DMSO/H_2O solution. The fluorescent effect of **L2**+Zn^{2+} is best when pH values get close to neutrality, which could have a similar explaination like **L2**+Al^{3+} .

The proposed mechanism

The low fluorescence of the free receptor may be attributed to a large extent of intramolecular charge transfer (ICT). Upon interaction with the target anaystes, the intramolecular charge transfer (ICT) changed following the principle of forming a stable structure. Hence, the chelation enhanced fluorescence (CHEF) process occured in the presence of the analysts, accompanying with a large Stokes shift. Moreover, a difference in the charge density of the cations and solvent effect are likely to affect the ICT mechanism. This may account for the different emission spectra of the probe upon interaction with Al^{3+} and Zn^{2+} in different solvent (Scheme 2).

Conclusions

In summary, we designed and synthesized a new fluorescent probe, **L2**, which selectively senses Al^{3+} and Zn^{2+} ions with a switch ON response in its fluorescence spectra. **L2** shows an prominent fluorescent selectivity toward Al^{3+} over other common metal ions in DMSO/H_2O HEPES buffer (10 mM, pH=7.4, 9:1, v/v) and shows an excellent fluorescent selectivity toward Zn^{2+} over other common metal ions in EtOH/H_2O HEPES buffer (10 mM, pH=7.4, 9:1, v/v). The detection limits for Al^{3+} and Zn^{2+} were found to be as low as 1.73×10^{-7} M and 6.36×10^{-8} M, respectively.

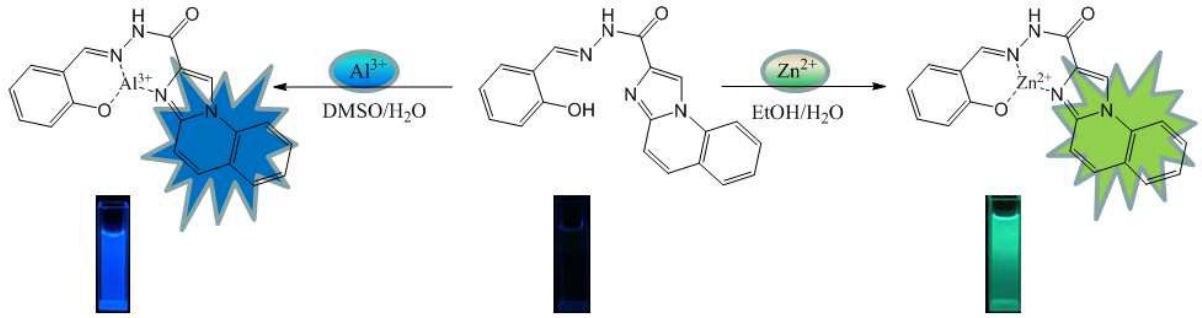

Scheme 2 The proposed mechanism of **L2** with Al^{3+} in DMSO and Zn^{2+} in EtOH.

Acknowledgements

The authors thank Henan Sanmenxia Aoke Chemical Industry Co., Ltd. for financial support.

References

1 Jing-can Qin, Zheng-yin Yang, Long Fan, Xiao-ying Cheng, Tian-rong Li and Bao-dui Wang, Anal. Methods., 2014, **6**, 7343.
2 V. K. Gupta, A. K. Jain and G. Maheshwari, Talanta, 2007, **72**, 1469-1473.
3 T. P. Flaten, Brain Research Bulletin, 2001, **55**, 187–196.
4 Sima Paul, Abhishek Manna and Shyamaprosad Goswami, Dalton Trans., 2015,44, 11805-11810.
5 K.H. Falchuk, Mol. Cell. Biochem.,1998, **188**, 41–48.
6 D.K. Perry, M.J. Smyth, H.R. Stennicke, G.S. Salvesen, P. Duriez, G.G. Poirier, and Y.A. Hannun, J. Biol. Chem., 1997, **272**, 18530–18533.
7 Math P. Cuajungco and Gordon J. Lees, neurobiology of disease, 1997, **4**, 137–169.
8 Pamela J. Fraker and Louis E. King, Annu. Rev. Nutr., 2004, **24**, 277–98.
9 C.F. Walker and R.E. Black, Annu. Rev. Nutr., 2004, **24**, 255 –275.
10 J.H. Weiss, S.L. Sensi, and J.Y. Koh, Trends Pharmacol. Sci., 2000, **21**, 395–401.
11 Bernard Valeur and Isabelle Leray, Coordination Chemistry Reviews, 2000, **205**, 3–40.
12 A. Ojida, I. Takashima, T. Kohira, H. Nonaka, I. Hamachi, J. Am. Chem. Soc., 2008, **130**, 12095–12101.
13 P.S. Hariharan, Natarajan Hari, and Savarimuthu Philip Anthony, Inorganic Chemistry Communications 2014, **48**, 1–4.
14 Keli Zhong, Mingjun Cai, Shuhua Hou, Yanjiang Bian, and Lijun Tang, Bull. Korean Chem. Soc., 2014, **35**, 489.
15 Zhong-Liang Gong, Bao-Xiang Zhao,Wei-Yong Liu, Hong-Shui Lv, Journal of Photochemistry and Photobiology A, 2011, **218**, 6–10.
16 Lijun Tang, Xin Dai, Keli Zhong, DiWu, XinWen, Sensors and Actuators B, 2014, **203**, 557–564.
17 Eun Joo Song, Hyun Kim, In Hong Hwang, Kyung Beom Kim, Ah Ram Kim Insup Nohb, and Cheal Kima, Sensors and Actuators B, 2014, **195**, 36–43.
18 Masayori Hagimori, Takashi Temma, Naoko Mizuyama, Takuhiro Uto, Yasuchika Yamaguchi, Yoshinori Tominaga, Takahiro Mukai, and Hideo Saji, Sensors and Actuators B, 2015, **213**, 45–52.
19 Aasif Helal , Mohammad Harun Or Rashid , Cheol-Ho Choi , and Hong-Seok Kim, Tetrahedron, 2012, **68**, 647-653.
20 Kang Shen, Xia Yang, Yixiang Cheng, and Chengjian Zhu, Tetrahedron, 2012, **68**, 5719-5723.
21 Hyungjoo Kim, Boddu Ananda Rao, Jong Woo Jeong, Sudipta Mallick,Sung-Min Kang, Joon Sig Choi, Chang-Soo Lee, and Young-A. Son, Sensors and Actuators B, 2015, **210**, 173–182.
22 Sudipto Dey, Shibashis Halder, Abhishek Mukherjee, Koushik Ghosh, and Partha Roy, Sensors and Actuators B, 2015, **215**, 196–205.
23 Ye Won Choi, Gyeong Jin Park, Yu Jeong Na, Hyun Yong Jo, Seul Ah Lee Ga Rim You, and Cheal Kim, Sensors and Actuators B, 2014, **194**, 343–352.
24 Junfeng Wang and Yi Pang, RSC Adv., 2014, 4, 5845-5848.
25 Xiaobo Huang, Qian Miao, Lu Wang, Jieming Jiao, Xianjing He, and Yixiang Cheng, Chin. J. Chem., 2013, **31**, 195–199.
26 Jing-can Qin, Zheng-yin Yang, Long Fan, Xiao-ying Cheng, Tian-rong Li, and Bao-dui Wang, Anal. Methods, 2014, **6**, 7343.
27 Barun Kumar Datta, Durairaj Thiyagarajan, Aiyagari Ramesh, and Gopal Das, Dalton Trans., 2015, **44**, 13093-13099.
28 Pengxuan Li, Xiaoyan Zhou, Ruoying Huang, Lizi Yang, Xiaoliang Tang, Wei Dou, Qianqian Zhao, and Weisheng Liu, Dalton Trans., 2014, **43**, 706.
29 Ajit Kumar Mahapatra, Saikat Kumar Manna, Chitrangada Das Mukhopadhyay, and Debasish Mandal, Sensors and Actuators B, 2014, **200**, 123–131.
30 Ye Won Choi, Jae Jun Lee and Cheal Kim, RSC Adv., 2015, **5**, 60796-60803.
31 Yuanyuan Yue, Qiao Dong, Yajie Zhang, Yangyang Suna and Yijun Gong, Anal. Methods, 2015, **7**, 5661-5666.
32 K. Velmurugan, A. Raman, Derin Don, Lijun Tang, S. Easwaramoorthi and R. Nandhakumar, RSC Adv., 2015, **5**, 44463-44469.
33 Joseph Ponniah S, Subrat Kumar Barik, Rosmita Borthakur, Arunabha Thakur, Bikash Garai, Sourita Janaa and Sundargopal Ghosh, RSC Adv., 2015, **5**, 15690-15694.
34 Oleg V. Larionov, David Stephens, Adelphe M. Mfuh, Hadi D. Arman, Anastasia S. Naumova, Gabriel Chavez and Behije Skenderi, Org. Biomol. Chem., 2014, **12**, 3026.
35 Jingjun Yin, Bangping Xiang, Mark A. Huffman, Conrad E. Raab, and Ian W. Davies, J. Org. Chem. 2007, **72**, 4554-4557.
36 Jacob A. Kaizerman, Matthew I. Gross, Yigong Ge, Sarah White, Wenhao Hu, Jian-Xin Duan, Eldon E. Baird, Kirk W.

Johnson, Richard D. Tanaka, Heinz E. Moser, and Roland W. Burli, J. Med. Chem., 2003, **46**, 3914-3929.

Abstract

A new chemsensor N'-[(2-hydroxyphenyl)methylidene]imidazo[1,2-a] quinoline-2-carbohydrazide (**L2**) was developed which could detect Al^{3+} in DMSO/H_2O HEPES buffer and detect Zn^{2+} in EtOH/H_2O HEPES buffer. The chemsensor exhibits high selectivity and sensitivity for sensing Al^{3+} and Zn^{2+} with a fluorescense "turn-on" mode.